Article

Not peer-reviewed version

Advanced Dynamic Thermal Vibration of Thick FGM Cylindrical Shells

C.C. Hong *

Posted Date: 2 February 2024

doi: 10.20944/preprints202402.0142.v1

Keywords: thick FGM; circular cylindrical shells; third-order shear deformation theory; TSDT; advanced thermal vibration; GDQ; nonlinear coefficient

Article

Advanced Dynamic Thermal Vibration of Thick FGM Cylindrical Shells

C.C. Hong [1,*]

[1] Department of Mechanical Engineering, Hsiuping University of Science and Technology, Taichung, 412-406 Taiwan, ROC; cchong@mail.hust.edu.tw

* Correspondence: cchong@mail.hust.edu.tw

Abstract: The thick functionally graded material (FGM) circular cylindrical shells with advanced varied shear correction coefficient and third-order shear deformation theory (TSDT) under advanced thermal vibration are studied by the method of generalized differential quadrature (GDQ). The coefficient of displacement model of TSDT is applied to derive the equations of motion for the thick FGM circular cylindrical shells. The stiffness in simpler forms of thick FGM circular cylindrical shells and temperature rise in linear expression of the heat conduction equation are used. The differential equations in dynamic equilibrium state of thick FGM circular cylindrical shells can be obtained and rewritten into displacements and shear rotations in partial derivative expressions under dynamic thermal loads in partial derivative expressions. Parametric effect studies including advanced nonlinear varied shear correction coefficient, nonlinear coefficient c_1 value, power law index and thermal temperature difference of external heating loads on the displacements and stresses of thick FGM cylindrical shells under thermal dynamic vibration are investigated.

Keywords: thick FGM; circular cylindrical shells; third-order shear deformation theory; TSDT; advanced thermal vibration; GDQ; nonlinear coefficient

1. Introduction

Usually the shear effect on the displacements and stresses were more considered in the thick thickness materials than in the thin one under every external loads. Some papers of functionally graded materials (FGMs) were investigated usually including the shear effect. Abouelregal et al. [1] in 2023 applied the Laplace transform and decoupling techniques to study the thermal vibration of spinning FGM isotropic piezoelectric rod. The effecting numerical results for non-homogeneous index in the displacement, temperature, electric potential and thermal stress were presented. The thermal stress variation was found in one of the most significant results want to be considered. In 2023, Tang et al. [2] used the radial integral boundary element method (RIBEM) to study the FGM plate under thermal shock loading. The numerical results of displacement, temperature and thermal stress were presented in the thick FGM plate. In 2022, Chen et al. [3] used the Rayleih–Ritz energy method with the first-order shear deformation theory (FSDT) of displacement models to investigate the vibration of FGM stepped cylindrical shell coupled with annular plate under thermal environment. The temperature-dependent constituent materials SUS304 and Si_3N_4 were used to study the transient responses of displacements. In 2022, Ramteke et al. [4] presented a nonlinear eigen- frequency responses with the higher-order shear deformation theory (HSDT) of displacement models for porous FGM shell panel under thermal environment by using the finite element method (FEM). In 2021, Saeedi et al. [5] applied differential quadrature (DQ) method to study the stresses distributions of thick FGM cylindrical shell with aluminum and silicon carbide under internal pressure and thermal loadings. In 2022, Gee and Hashemi [6] used the dynamic finite element (DFE) method to investigate the numerical results of natural frequencies for the FGM beams. In 2019, Khoshgoftar [7] used the virtual work principle and second-order shear

 doi:10.20944/preprints202402.0142.v1

deformation theory (SSDT) of displacement models to obtain the numerical displacement results of axis-symmetric thick FGM shells under non-uniform pressure. In 2019, Trinh and Kim [8] presented the nonlinear stability of moderately thick FGM sandwich shells supported by elastic foundations under thermo-mechanical loadings by using the Bubnov–Galerkin procedure, harmonic balance principle and FSDT of displacement models. The numerical solutions for thermal buckling load are obtained. In 2017, Nejad et al. [9] presented a review for some models used in the solving methods, elasticity theories and shear deformation theories used for the thick FGM cylindrical and conical shells.

Some generalized differential quadrature (GDQ) computational results with nonlinear displacement third-order shear deformation theory (TSDT), thermal temperature of environment and external heating loads were presented for the thermal vibrations of FGMs. Hong [10] in 2023 studied the GDQ solutions of thick FGM plates with the effects of TSDT model but not in function of nonlinear coefficient c_1 term of TSDT model. In 2022, Hong [11] presented the dynamic advanced GDQ solutions of thick FGM plates under thermal vibration with the effects of TSDT and advanced shear factor that was in function of c_1 term of TSDT model, FGM power law index and environment temperature, but not in function of total thickness. Hong [12] in 2022 presented the GDQ solutions of thick FGM circular cylindrical shells under thermal vibration with the effects of TSDT and varied shear factor that was not in function of c_1 term of TSDT model. Hong [13] in 2022 studied the advanced GDQ results of thick FGM plates-cylindrical shells under thermal vibration with the effects of TSDT and advanced shear factor that was in function of c_1 term of TSDT model, FGM power law index and environment temperature, but not in function of total thickness of plates-cylindrical shells. The further study now providing the GDQ vibration results of stresses and displacements with the effects of TSDT, advanced varied shear correction coefficient, environment temperature and power law index.

2. Formulation

Two constituent material FGM circular cylindrical shell is studied in **Figure 1**, in which the parameter of h_1 denotes the inner layer thickness of constituent material 1, h_2 denotes the outer layer thickness of constituent material 2, L denotes the axial length, and h^* denotes the total thickness. The material properties in power-law function are studied and parameter of E_{fgm} denotes Young's modulus in standard variation form of FGMs, R_n denotes power law index, and ν_{fgm} denotes Poisson's ratios of FGMs that is assumed in the simple average form as follows [10],

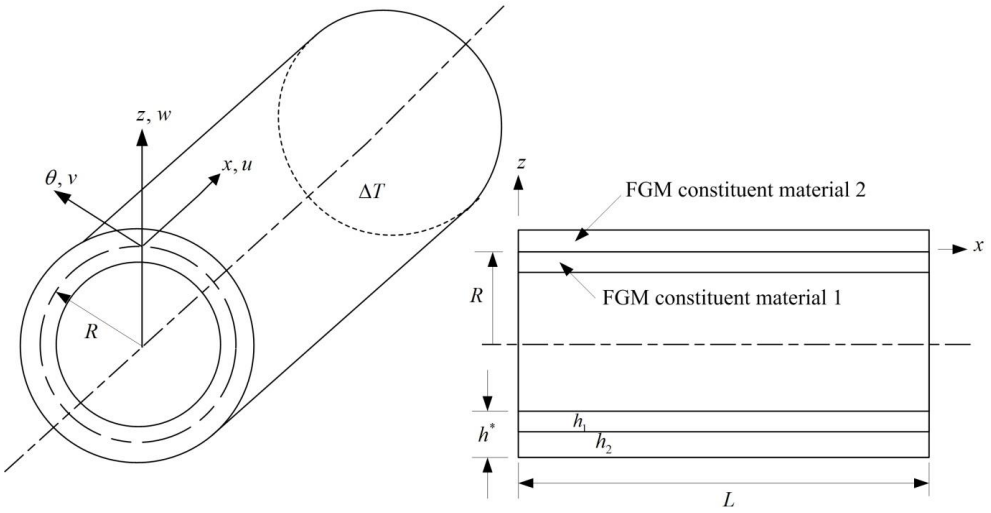

Figure 1. Two constituent material of thick FGM circular cylindrical shells.

$$E_{fgm} = (E_2 - E_1)\left(\frac{z+\frac{h^*}{2}}{h^*}\right)^{R_n} + E_1 \quad (1a)$$

$$\nu_{fgm} = (\nu_1 + \nu_2)/2 \quad (1b)$$

 doi:10.20944/preprints202402.0142.v1

where E_1 and E_2 are the Young's modulus, ν_1 and ν_2 are the Poisson's ratios of the constituent material 1 and material 2, respectively in the FGMs.

The properties P_i of individual constituent material of FGMs, e.g., E_1, E_2, ν_1 and ν_2 are in functions of environment temperature T can be calculated by the following form,

$$P_i = P_0(P_{-1}T^{-1} + 1 + P_1T + P_2T^2 + P_3T^3) \quad (1c)$$

in which P_0, P_{-1}, P_1, P_2 and P_3 are the temperature coefficients.

The time dependent displacement vector $\vec{\mathbf{u}}$ of thick FGM circular cylindrical shells are studied in the nonlinear of z^3 form with nonlinear coefficient c_1 term of TSDT equations [12,14] as follows,

$$\mathbf{u} = \mathbf{u_0} + z\,\boldsymbol{\phi} - c_1 z^3(\boldsymbol{\phi} + \frac{\partial w}{\partial \mathbf{x}}) \quad (2)$$

where $\mathbf{u} = [u, v, w]^{\mathrm{t}}$, $\mathbf{u_0} = [u_0(x,\theta,t), v_0(x,\theta,t), w(x,\theta,t)]^{\mathrm{t}}$, $\boldsymbol{\phi} = [\phi_x(x,\theta,t), \phi_\theta(x,\theta,t), 0]^{\mathrm{t}}$, $c_1 = 4/(3h^{*2})$ and $\partial\mathbf{x} = [\partial x, R\partial\theta, \partial z]^{\mathrm{t}}$, in which t denotes the time, u and v denote respectively the tangential displacements in the direction of x and θ axes. u_0 and v_0 denote respectively the tangential displacements in the direction of x and θ axes, w denotes the transverse displacement in the direction of z axis in the middle-plane of FGM shells. ϕ_x and ϕ_θ denote the shear rotations. R denotes the radius of middle-surface in FGM shells. The superscript t is operating the transpose of vector.

The stress vector $\boldsymbol{\sigma}$ in the thick FGM circular cylindrical shells under external heating loads with temperature difference ΔT for the k th constituent layer are studied in the following equations [15],

$$\boldsymbol{\sigma} = \bar{\mathbf{Q}}\,(\boldsymbol{\varepsilon} - \boldsymbol{\alpha}\,\Delta T) \quad (3)$$

where $\boldsymbol{\sigma} = [\sigma_x, \sigma_\theta, \sigma_{x\theta}, \sigma_{\theta z}, \sigma_{xz}]^{\mathrm{t}}$, $\boldsymbol{\varepsilon} = [\varepsilon_x, \varepsilon_\theta, \varepsilon_{x\theta}, \varepsilon_{\theta z}, \varepsilon_{xz}]^{\mathrm{t}}$, $\boldsymbol{\alpha} = [\alpha_x, \alpha_\theta, \alpha_{x\theta}, 0, 0]^{\mathrm{t}}$ and

$$\bar{\mathbf{Q}} = \begin{bmatrix} \bar{Q}_{11} & \bar{Q}_{12} & \bar{Q}_{16} & 0 & 0 \\ \bar{Q}_{12} & \bar{Q}_{22} & \bar{Q}_{26} & 0 & 0 \\ \bar{Q}_{16} & \bar{Q}_{26} & \bar{Q}_{66} & 0 & 0 \\ 0 & 0 & 0 & \bar{Q}_{44} & \bar{Q}_{45} \\ 0 & 0 & 0 & \bar{Q}_{45} & \bar{Q}_{55} \end{bmatrix}$$

in which σ_x and σ_θ are the normal stresses, $\sigma_{x\theta}, \sigma_{\theta z}$ and σ_{xz} are the shear stresses. $\varepsilon_x, \varepsilon_\theta$ and $\varepsilon_{x\theta}$ are in-plane strains, $\varepsilon_{\theta z}$ and ε_{xz} are shear strains can't negligible for thick shells. α_x and α_θ are thermal expansion coefficients, $\alpha_{x\theta}$ is the thermal shear coefficient. $\bar{Q}_{ij}$ with subscripts i, j=1,2,4,5 and 6 are the stiffness of FGM shells.

The advanced varied shear correction coefficient k_α can be used as a coefficient in the following stiffness $\bar{Q}_{ij}$ integral equations $A_{i^s j^s}$, $B_{i^s j^s}$, $D_{i^s j^s}$, $E_{i^s j^s}$, $F_{i^s j^s}$, $H_{i^s j^s}$ and $A_{i^* j^*}$, $B_{i^* j^*}$, $D_{i^* j^*}$, $E_{i^* j^*}$, $F_{i^* j^*}$, $H_{i^* j^*}$ with subscripts i^*, j^*=4,5 when $\varepsilon_{\theta z}$ and ε_{xz} can't negligible in thick shells, also for subscripts i^s, j^s=1,2,6 when $\varepsilon_x, \varepsilon_\theta$ and $\varepsilon_{x\theta}$ are applied.

$$(A_{i^s j^s},\ B_{i^s j^s},\ D_{i^s j^s}, E_{i^s j^s},\ F_{i^s j^s},\ H_{i^s j^s}) = \int_{-\frac{h^*}{2}}^{\frac{h^*}{2}} \bar{Q}_{i^s j^s}\,(1, z, z^2, z^3, z^4, z^6)\mathrm{d}z \quad (4a)$$

$$(A_{i^* j^*},\ B_{i^* j^*},\ D_{i^* j^*}, E_{i^* j^*},\ F_{i^* j^*},\ H_{i^* j^*}) = \int_{-\frac{h^*}{2}}^{\frac{h^*}{2}} k_\alpha \bar{Q}_{i^* j^*}\,(1, z, z^2, z^3, z^4, z^5)\mathrm{d}z \quad (4b)$$

where simple forms of $\bar{Q}_{i^s j^s}$ and $\bar{Q}_{i^* j^*}$ are used in the following with z/R term cannot be neglected [16], $\bar{Q}_{11} = \bar{Q}_{22} = \frac{E_{fgm}}{1-\nu_{fgm}^2}$, $\bar{Q}_{12} = \bar{Q}_{21} = \frac{\nu_{fgm}E_{fgm}}{\left(1+\frac{z}{R}\right)(1-\nu_{fgm}^2)}$, $\bar{Q}_{44} = \frac{E_{fgm}}{2(1+\nu_{fgm})}$, $\bar{Q}_{55} = \bar{Q}_{66} = \frac{E_{fgm}}{2\left(1+\frac{z}{R}\right)(1+\nu_{fgm})}$ and $\bar{Q}_{16} = \bar{Q}_{26} = \bar{Q}_{45} = 0$.

And the advanced k_α expression can be derived and expressed in the following equation by using the total strain energy principle to apply [11],

$$k_\alpha = \frac{1}{h^*}\frac{FGMZSV}{FGMZIV} \quad (4c)$$

in which $FGMZSV = (FGMZS - c_1 FGMZSN)^2$, $FGMZIV = FGMZI - 2c_1 FGMZIV1 + {c_1}^2 FGMZIV2$ with parameters *FGMZS*, *FGMZSN*, *FGMZI*, *FGMZIV1* and *FGMZIV2* are in functions of E_1, E_2, h^* and R_n. The calculated values of nonlinear advanced k_α are usually functions of c_1, R_n and T.

The ΔT time dependent expression can be studied between the FGM shell and curing area under external heating loads by using the following equation in linear of z,

 doi:10.20944/preprints202402.0142.v1

$$\Delta T = \frac{z}{h^*} T_1 \quad (5a)$$

where temperature parameter $T_1 = T_1(x,\theta,t)$, also the simple form heat conduction equation in cylindrical axes is used in the following [10],

$$K\left(\frac{\partial^2 \Delta T}{\partial x^2} + \frac{\partial^2 \Delta T}{R^2 \partial \theta^2} + \frac{\partial^2 \Delta T}{\partial z^2}\right) = \frac{\partial \Delta T}{\partial t} \quad (5b)$$

in which $K = \kappa_{fgm}/(\rho_{fgm} C_{v_{fgm}})$, κ_{fgm} denotes the thermal conductivity of FGMs, ρ_{fgm} denotes the density of FGMs, $C_{v_{fgm}}$ denotes the specific heat of FGMs, they are all assumed in the simple average property form of constituent material 1 and 2, e.g., $\rho_{fgm} = (\rho_1 + \rho_2)/2$ with ρ_1, ρ_2 is density of FGM constituent material 1 and 2, respectively.

The dynamic equations of motion in the thick FGM cylindrical shells with TSDT are given in the following that can be derived by using the generalized Hamilton total energy principle [13],

$$\frac{\partial N_{xx}}{\partial x} + \frac{1}{R}\frac{\partial N_{x\theta}}{\partial \theta} = I_0 \frac{\partial^2 u_0}{\partial t^2} + J_1 \frac{\partial^2 \phi_x}{\partial t^2} - c_1 I_3 \frac{\partial^2}{\partial t^2}\left(\frac{\partial w}{\partial x}\right) \quad (6a)$$

$$\frac{\partial N_{x\theta}}{\partial x} + \frac{1}{R}\frac{\partial N_{\theta\theta}}{\partial \theta} = I_0 \frac{\partial^2 v_0}{\partial t^2} + J_1 \frac{\partial^2 \phi_\theta}{\partial t^2} - c_1 I_3 \frac{\partial^2}{\partial t^2}\left(\frac{1}{R}\frac{\partial w}{\partial \theta}\right) \quad (6b)$$

$$\frac{\partial \overline{Q}_x}{\partial x} + \frac{1}{R}\frac{\partial \overline{Q}_\theta}{\partial \theta} + c_1\left(\frac{\partial^2 P_{xx}}{\partial x^2} + \frac{2}{R}\frac{\partial^2 P_{x\theta}}{\partial x \partial \theta} + \frac{1}{R^2}\frac{\partial^2 P_{\theta\theta}}{\partial \theta^2}\right) + q = I_0 \frac{\partial^2 w}{\partial t^2} - c_1^2 I_6 \frac{\partial^2}{\partial t^2}\left(\frac{\partial^2 w}{\partial x^2} + \frac{1}{R^2}\frac{\partial^2 w}{\partial \theta^2}\right)$$
$$+ c_1\left[I_3 \frac{\partial^2}{\partial t^2}\left(\frac{\partial u_0}{\partial x} + \frac{1}{R}\frac{\partial v_0}{\partial \theta}\right) + J_4 \frac{\partial^2}{\partial t^2}\left(\frac{\partial \phi_x}{\partial x} + \frac{1}{R}\frac{\partial \phi_\theta}{\partial \theta}\right)\right] \quad (6c)$$

$$\frac{\partial \overline{M}_{xx}}{\partial x} + \frac{1}{R}\frac{\partial \overline{M}_{x\theta}}{\partial \theta} - \overline{Q}_x = \frac{\partial^2}{\partial t^2}\left(J_1 u_0 + K_2 \phi_x - c_1 J_4 \frac{\partial w}{\partial x}\right) \quad (6d)$$

$$\frac{\partial \overline{M}_{x\theta}}{\partial x} + \frac{1}{R}\frac{\partial \overline{M}_{\theta\theta}}{\partial \theta} - \overline{Q}_\theta = \frac{\partial^2}{\partial t^2}\left(J_1 v_0 + K_2 \phi_\theta - c_1 J_4 \frac{1}{R}\frac{\partial w}{\partial \theta}\right) \quad (6e)$$

where $\overline{M}_{\alpha\beta} = M_{\alpha\beta} - c_1 P_{\alpha\beta}$, $\overline{Q}_\alpha = Q_\alpha - 3c_1 R_\alpha$, subscripts $(\alpha, \beta = x, \theta)$, $\begin{Bmatrix} N_{xx} \\ N_{\theta\theta} \\ N_{x\theta} \end{Bmatrix} = \int_{-\frac{h^*}{2}}^{\frac{h^*}{2}} \begin{Bmatrix} \sigma_x \\ \sigma_\theta \\ \sigma_{x\theta} \end{Bmatrix} dz$, $\begin{Bmatrix} M_{xx} \\ M_{\theta\theta} \\ M_{x\theta} \end{Bmatrix} = \int_{-\frac{h^*}{2}}^{\frac{h^*}{2}} \begin{Bmatrix} \sigma_x \\ \sigma_\theta \\ \sigma_{x\theta} \end{Bmatrix} z\, dz$, $\begin{Bmatrix} P_{xx} \\ P_{\theta\theta} \\ P_{x\theta} \end{Bmatrix} = \int_{-\frac{h^*}{2}}^{\frac{h^*}{2}} \begin{Bmatrix} \sigma_x \\ \sigma_\theta \\ \sigma_{x\theta} \end{Bmatrix} z^3\, dz$, $\begin{Bmatrix} R_\theta \\ R_x \end{Bmatrix} = \int_{-\frac{h^*}{2}}^{\frac{h^*}{2}} \begin{Bmatrix} \sigma_{\theta z} \\ \sigma_{xz} \end{Bmatrix} z^2\, dz$, $\begin{Bmatrix} Q_\theta \\ Q_x \end{Bmatrix} = \int_{-\frac{h^*}{2}}^{\frac{h^*}{2}} \begin{Bmatrix} \sigma_{\theta z} \\ \sigma_{xz} \end{Bmatrix} dz$, q is external pressure load, $I_i = \sum_{k=1}^{N^*} \int_k^{k+1} \rho^{(k)} z^i dz$, ($i$= 0, 1, 2,…,6), with N^* denotes the constituent layers total number, $\rho^{(k)}$ denotes the density of superscript k th constituent layer, $J_i = I_i - c_1 I_{i+2}$, in which subscript i=1, 4 and $K_2 = I_2 - 2c_1 I_4 + c_1^2 I_6$. And assumed strain-displacement relations with $\frac{\partial v_0}{\partial z} = \frac{-v_0}{R}$, $\frac{\partial u_0}{\partial z} = \frac{-u_0}{R}$ and $\frac{\partial w}{\partial z} = \frac{\partial \phi_x}{\partial z} = \frac{\partial \phi_\theta}{\partial z} = 0$ are used as follows,

$$\varepsilon_x = \frac{\partial u}{\partial x} + \frac{1}{2}\left(\frac{\partial w}{\partial x}\right)^2 = \frac{\partial u_0}{\partial x} + z\frac{\partial \phi_x}{\partial x} - c_1 z^3\left(\frac{\partial \phi_x}{\partial x} + \frac{\partial^2 w}{\partial x^2}\right) + \frac{1}{2}\left(\frac{\partial w}{\partial x}\right)^2 \quad (7a)$$

$$\varepsilon_\theta = \frac{1}{R}\frac{\partial v}{\partial \theta} + \frac{1}{2}\left(\frac{1}{R}\frac{\partial w}{\partial \theta}\right)^2 = \frac{1}{R}\frac{\partial v_0}{\partial \theta} + z\frac{1}{R}\frac{\partial \phi_\theta}{\partial \theta} - c_1 z^3\left(\frac{1}{R}\frac{\partial \phi_\theta}{\partial \theta} + \frac{1}{R^2}\frac{\partial^2 w}{\partial \theta^2}\right) + \frac{1}{2}\frac{1}{R^2}\left(\frac{\partial w}{\partial \theta}\right)^2 \quad (7b)$$

$$\varepsilon_{zz} = 0 \quad (7c)$$

$$\varepsilon_{x\theta} = \frac{1}{R}\frac{\partial u}{\partial \theta} + \frac{\partial v}{\partial x} + \left(\frac{\partial w}{\partial x}\right)\left(\frac{1}{R}\frac{\partial w}{\partial \theta}\right) = \frac{1}{R}\left[\frac{\partial u_0}{\partial \theta} + z\frac{\partial \phi_x}{\partial \theta} - c_1 z^3\left(\frac{\partial \phi_x}{\partial \theta} + \frac{\partial^2 w}{\partial x \partial \theta}\right)\right]$$
$$+ \frac{\partial v_0}{\partial x} + z\frac{\partial \phi_\theta}{\partial x} - c_1 z^3\left(\frac{\partial \phi_\theta}{\partial x} + \frac{1}{R}\frac{\partial^2 w}{\partial x \partial \theta}\right) + \left(\frac{\partial w}{\partial x}\right)\left(\frac{1}{R}\frac{\partial w}{\partial \theta}\right) \quad (7d)$$

$$\varepsilon_{\theta z} = \frac{\partial v}{\partial z} + \frac{1}{R}\frac{\partial w}{\partial \theta} = \frac{-v_0}{R} + \phi_\theta - 3c_1 z^2\left(\phi_\theta + \frac{1}{R}\frac{\partial w}{\partial \theta}\right) + \frac{1}{R}\frac{\partial w}{\partial \theta} \quad (7e)$$

 doi:10.20944/preprints202402.0142.v1

$$\varepsilon_{xz} = \frac{\partial u}{\partial z} + \frac{\partial w}{\partial x} = \frac{-u_0}{R} + \phi_x - 3c_1 z^2(\phi_x + \frac{\partial w}{\partial x}) + \frac{\partial w}{\partial x} \quad (7f)$$

Substitute eqs. (3) and (7) into eq. (6), the dynamic equilibrium differential equations in the cylindrical coordinates of thick FGM circular cylindrical shells in terms of partial derivatives of u_0, v_0, w, ϕ_x and ϕ_θ with TSDT under partial derivatives of external loads can be written in matrix forms as follows [13].

$$\mathbf{HM}[\frac{\partial^4 w}{\partial x^4} \ \frac{1}{R}\frac{\partial^4 w}{\partial x^3 \partial\theta} \ \frac{1}{R^2}\frac{\partial^4 w}{\partial x^2 \partial\theta^2} \ \frac{1}{R^3}\frac{\partial^4 w}{\partial x \partial\theta^3} \ \frac{1}{R^4}\frac{\partial^4 w}{\partial\theta^4}]^t +$$
$$\mathbf{EM}[\frac{\partial^3 u_0}{\partial x^3} \ \frac{1}{R}\frac{\partial^3 u_0}{\partial x^2\partial\theta} \ \frac{1}{R^2}\frac{\partial^3 u_0}{\partial x\partial\theta^2} \ \frac{1}{R^3}\frac{\partial^3 u_0}{\partial\theta^3} \ \frac{\partial^3 v_0}{\partial x^3} \ \frac{1}{R}\frac{\partial^3 v_0}{\partial x^2\partial\theta} \ \frac{1}{R^2}\frac{\partial^3 v_0}{\partial x\partial\theta^2} \ \frac{1}{R^3}\frac{\partial^3 v_0}{\partial\theta^3}$$
$$\frac{\partial^3 w}{\partial x^3} \ \frac{1}{R}\frac{\partial^3 w}{\partial x^2\partial\theta} \ \frac{1}{R^2}\frac{\partial^3 w}{\partial x\partial\theta^2} \ \frac{1}{R^3}\frac{\partial^3 w}{\partial\theta^3}]^t +$$
$$\mathbf{FM}[\frac{\partial^3 \phi_x}{\partial x^3} \ \frac{1}{R}\frac{\partial^3 \phi_x}{\partial x^2\partial\theta} \ \frac{1}{R^2}\frac{\partial^3 \phi_x}{\partial x\partial\theta^2} \ \frac{1}{R^3}\frac{\partial^3 \phi_x}{\partial\theta^3} \ \frac{\partial^3 \phi_\theta}{\partial x^3} \ \frac{1}{R}\frac{\partial^3 \phi_\theta}{\partial x^2\partial\theta} \ \frac{1}{R^2}\frac{\partial^3 \phi_\theta}{\partial x\partial\theta^2} \ \frac{1}{R^3}\frac{\partial^3 \phi_\theta}{\partial\theta^3}]^t +$$
$$\mathbf{AM}[\frac{\partial^2 u_0}{\partial x^2} \ \frac{1}{R}\frac{\partial^2 u_0}{\partial x\partial\theta} \ \frac{1}{R^2}\frac{\partial^2 u_0}{\partial\theta^2} \ \frac{\partial^2 v_0}{\partial x^2} \ \frac{1}{R}\frac{\partial^2 v_0}{\partial x\partial\theta} \ \frac{1}{R^2}\frac{\partial^2 v_0}{\partial\theta^2} \ \frac{\partial^2 w}{\partial x^2} \ \frac{1}{R}\frac{\partial^2 w}{\partial x\partial\theta} \ \frac{1}{R^2}\frac{\partial^2 w}{\partial\theta^2}]^t +$$
$$\mathbf{BM}[\frac{\partial^2 \phi_x}{\partial x^2} \ \frac{1}{R}\frac{\partial^2 \phi_x}{\partial x\partial\theta} \ \frac{1}{R^2}\frac{\partial^2 \phi_x}{\partial\theta^2} \ \frac{\partial^2 \phi_\theta}{\partial x^2} \ \frac{1}{R}\frac{\partial^2 \phi_\theta}{\partial x\partial\theta} \ \frac{1}{R^2}\frac{\partial^2 \phi_\theta}{\partial\theta^2}]^t +$$
$$\mathbf{KE}[\frac{\partial u_0}{\partial x} \ \frac{1}{R}\frac{\partial u_0}{\partial\theta} \ \frac{\partial v_0}{\partial x} \ \frac{1}{R}\frac{\partial v_0}{\partial\theta} \ \frac{\partial w}{\partial x} \ \frac{1}{R}\frac{\partial w}{\partial\theta} \ \frac{\partial \phi_x}{\partial x} \ \frac{1}{R}\frac{\partial \phi_x}{\partial\theta} \ \frac{\partial \phi_\theta}{\partial x} \ \frac{1}{R}\frac{\partial \phi_\theta}{\partial\theta}]^t +$$
$$\mathbf{FQ}\,[u_0 \ v_0 \ w \ \phi_x \ \phi_\theta]^t = [f_1 \ f_2 \ f_3 \ f_4 \ f_5]^t \quad (8)$$

where $\mathbf{HM} = [\mathrm{HM}_{ij}]$ is a 5 by 5 matrix, $\mathbf{EM} = [\mathrm{EM}_{ij}]$ is a 5 by 12 matrix, $\mathbf{FM} = [\mathrm{FM}_{ij}]$ is a 5 by 8 matrix, $\mathbf{AM} = [\mathrm{AM}_{ij}]$ is a 5 by 9 matrix, $\mathbf{BM} = [\mathrm{BM}_{ij}]$ is a 5 by 6 matrix, $\mathbf{KE} = [\mathrm{KE}_{ij}]$ is a 5 by 10 matrix, $\mathbf{FQ} = [\mathrm{FQ}_{ij}]$ is a 5 by 5 matrix, for more details of these matrices are expressed in the section **Appendix A**.

$$f_1 = \frac{\partial \overline{N}_{xx}}{\partial x} + \frac{1}{R}\frac{\partial \overline{N}_{x\theta}}{\partial\theta} + p_1, \quad f_2 = \frac{\partial \overline{N}_{x\theta}}{\partial x} + \frac{1}{R}\frac{\partial \overline{N}_{\theta\theta}}{\partial\theta} + p_2,$$

$$f_3 = -q + c_1(\frac{\partial^2 \overline{P}_{xx}}{\partial x^2} + \frac{2}{R}\frac{\partial^2 \overline{P}_{x\theta}}{\partial x\partial\theta} + \frac{1}{R^2}\frac{\partial^2 \overline{P}_{\theta\theta}}{\partial\theta^2}), \quad f_4 = \frac{\partial \tilde{\overline{M}}_{xx}}{\partial x} + \frac{1}{R}\frac{\partial \tilde{\overline{M}}_{x\theta}}{\partial\theta} - c_1(\frac{\partial \overline{P}_{xx}}{\partial x} + \frac{1}{R}\frac{\partial \overline{P}_{x\theta}}{\partial\theta})),$$

$$f_5 = \frac{\partial \tilde{\overline{M}}_{x\theta}}{\partial x} + \frac{1}{R}\frac{\partial \tilde{\overline{M}}_{\theta\theta}}{\partial\theta} - c_1(\frac{\partial \overline{P}_{x\theta}}{\partial x} + \frac{1}{R}\frac{\partial \overline{P}_{\theta\theta}}{\partial\theta}), \text{ with}$$

$$(\overline{N}_{xx}, \tilde{\overline{M}}_{xx}, \overline{P}_{xx}) = \int_{-\frac{h^*}{2}}^{\frac{h^*}{2}} (\overline{Q}_{11}\alpha_x + \overline{Q}_{12}\alpha_\theta + \overline{Q}_{16}\alpha_{x\theta})\Delta T(1, z, z^3)dz,$$

$$(\overline{N}_{\theta\theta}, \tilde{\overline{M}}_{\theta\theta}, \overline{P}_{\theta\theta}) = \int_{-\frac{h^*}{2}}^{\frac{h^*}{2}} (\overline{Q}_{12}\alpha_x + \overline{Q}_{22}\alpha_\theta + \overline{Q}_{26}\alpha_{x\theta})\Delta T(1, z, z^3)dz,$$

$$(\overline{N}_{x\theta}, \tilde{\overline{M}}_{x\theta}, \overline{P}_{x\theta}) = \int_{-\frac{h^*}{2}}^{\frac{h^*}{2}} (\overline{Q}_{16}\alpha_x + \overline{Q}_{26}\alpha_\theta + \overline{Q}_{66}\alpha_{x\theta})\Delta T(1, z, z^3)dz,$$

in which p_1 and p_2 are external in-plane distributed forces in x and θ direction respectively.

By using the GDQ numerical method to solve the equation (8) for the thick FGM circular cylindrical shells under time sinusoidal vibrations of displacement, shear rotations and thermal temperature difference of external heating loads only, i.e., $p_1 = p_2 = q = 0$ are studied as follows,

$$u_0(x,\theta,t) = u_0(x,\theta)\sin(\omega_{mn}t) \quad (9a)$$
$$v_0(x,\theta,t) = v_0(x,\theta)\sin(\omega_{mn}t) \quad (9b)$$
$$w(x,\theta,t) = w(x,\theta)\sin(\omega_{mn}t) \quad (9c)$$
$$\phi_x(x,\theta,t) = \phi_x(x,\theta)\sin(\omega_{mn}t) \quad (9d)$$
$$\phi_\theta(x,\theta,t) = \phi_\theta(x,\theta)\sin(\omega_{mn}t) \quad (9e)$$
$$\Delta T = \frac{z}{h^*}\bar{T}_1 \sin(\pi x/L)\sin(\pi\theta/R)\sin(\gamma t) \quad (9f)$$

 doi:10.20944/preprints202402.0142.v1

where ω_{mn} denotes the natural frequency with subscripts m, n denote the mode shape numbers of FGMs, γ denotes the applied heat flux frequency, $\bar{T}_1$ denotes the temperature amplitude.

For more detail procedures used in GDQ numerical method can be referred [10], the GDQ dynamic discrete equations could be obtained and expressed into the matrix equation as follows for a interior grid point at subscripts (i, j) in the computation,

$$[A][W^*] = [B] \quad (10)$$

in which $[A]$ denotes the coefficient matrix with dimension of N^{**} by N^{**} ($\mathrm{N}^{**} = 5(N-2)(\mathrm{M}-2)$) contains ($A_{i^s j^s}$, $B_{i^s j^s}$, $D_{i^s j^s}$, $E_{i^s j^s}$, $F_{i^s j^s}$, $H_{i^s j^s}$ and $A_{i^* j^*}$, $B_{i^* j^*}$, $D_{i^* j^*}$, $E_{i^* j^*}$, $F_{i^* j^*}$, $H_{i^* j^*}$) and weighting parameters ($A_{i,l}^{(m)}, B_{j,m}^{(m)}$) for the superscript m th-order derivative of the functions, e.g., $u_0(x,\theta)$, $v_0(x,\theta)$, $w(x,\theta)$, $\phi_x(x,\theta)$, $\phi_\theta(x,\theta)$, $\bar{N}_{xx}$, $\bar{N}_{x\theta}$, $\bar{N}_{\theta\theta}$, $\bar{P}_{xx}$, $\bar{P}_{x\theta}$, $\bar{P}_{\theta\theta}$, $\bar{\bar{M}}_{xx}$, $\bar{\bar{M}}_{x\theta}$ and $\bar{\bar{M}}_{\theta\theta}$ with respect to the x and θ directions.

$$[W^*] = [U_{2,2}, U_{2,3}, \cdots, U_{2,M-1}, \cdots, U_{N-1,2}, U_{N-1,3}, \cdots, U_{N-1,M-1},$$
$$V_{2,2}, V_{2,3}, \cdots, V_{2,M-1}, \cdots, V_{N-1,2}, V_{N-1,3}, \cdots, V_{N-1,M-1},$$
$$W_{2,2}, W_{2,3}, \cdots, W_{2,M-1}, \cdots, W_{N-1,2}, W_{N-1,3}, \cdots, W_{N-1,M-1},$$
$$\phi_{x_{2,2}}, \phi_{x_{2,3}}, \cdots, \phi_{x_{2,M-1}}, \cdots, \phi_{x_{N-1,2}}, \phi_{x_{N-1,3}}, \cdots, \phi_{x_{N-1,M-1}},$$
$$\phi_{\theta_{2,2}}, \phi_{\theta_{2,3}}, \cdots, \phi_{\theta_{2,M-1}}, \cdots, \phi_{\theta_{N-1,2}}, \phi_{\theta_{N-1,3}}, \cdots, \phi_{\theta_{N-1,M-1}}]^{\mathrm{t}}$$

is a N^{**}th-order unknown column vector, in which non-dimensional parameters $U = u_0/L$, $V = v_0/R$ and $W = w/h^*$ are used for column vector $[W^*]$ and $[B] = [F_1 \cdots F_1, F_2 \cdots F_2, F_3 \cdots F_3, F_4 \cdots F_4, F_5 \cdots F_5]^{\mathrm{t}}$ is a N^{**}th-order row external loads vector, in which

$$F_1 = \left(\frac{1}{L}\sum_{l=1}^{N} A_{i,l}^{(1)} \bar{N}_{xx_{l,j}} + \frac{1}{R}\sum_{m=1}^{M} B_{j,m}^{(1)} \bar{N}_{x\theta_{i,m}}\right)\sin(\gamma t),$$
$$F_2 = \left(\frac{1}{L}\sum_{l=1}^{N} A_{i,l}^{(1)} \bar{N}_{x\theta_{l,j}} + \frac{1}{R}\sum_{m=1}^{M} B_{j,m}^{(1)} \bar{N}_{\theta\theta_{i,m}}\right)\sin(\gamma t),$$
$$F_3 = c_1\left(\frac{1}{L^2}\sum_{l=1}^{N} A_{i,l}^{(2)} \bar{P}_{xx_{l,j}} + \frac{2}{LR}\sum_{l=1}^{N} A_{i,l}^{(1)}\sum_{m=1}^{M} B_{j,m}^{(1)} \bar{P}_{x\theta_{l,m}} + \frac{1}{R^2}\sum_{m=1}^{M} B_{j,m}^{(2)} \bar{P}_{\theta\theta_{i,m}}\right)\sin(\gamma t),$$
$$F_4 = \left(\frac{1}{L}\sum_{l=1}^{N} A_{i,l}^{(1)} \bar{\bar{M}}_{xx_{l,j}} + \frac{1}{R}\sum_{m=1}^{M} B_{j,m}^{(1)} \bar{\bar{M}}_{x\theta_{i,m}}\right)\sin(\gamma t) + c_1$$
$$\left(\frac{1}{L}\sum_{l=1}^{N} A_{i,l}^{(1)} \bar{P}_{xx_{l,j}} + \frac{1}{R}\sum_{m=1}^{M} B_{j,m}^{(1)} \bar{P}_{x\theta_{i,m}}\right)\sin(\gamma t)$$
$$F_5 = \left(\frac{1}{L}\sum_{l=1}^{N} A_{i,l}^{(1)} \bar{\bar{M}}_{x\theta_{l,j}} + \frac{1}{R}\sum_{m=1}^{M} B_{j,m}^{(1)} \bar{\bar{M}}_{\theta\theta_{i,m}}\right)\sin(\gamma t) + c_1$$
$$\left(\frac{1}{L}\sum_{l=1}^{N} A_{i,l}^{(1)} \bar{P}_{x\theta_{l,j}} + \frac{1}{R}\sum_{m=1}^{M} B_{j,m}^{(1)} \bar{P}_{\theta\theta_{i,m}}\right)\sin(\gamma t)$$

Thus the unknown column vector $[W^*]$ can be solved and obtained by computer programs. Also the inter-laminar stress $\boldsymbol{\sigma}$ in the k th constituent layer could be obtained.

3. Some numerical results

The x_i and θ_j coordinates for grid N and M in the computation of thick FGM circular cylindrical shells are applied as follows to obtain the thermal vibration GDQ results of advanced k_α with shells constituent layers in ($0^\circ/0^\circ$) under four sides simply supported boundary condition.

$$x_i = 0.5[1 - \cos\left(\frac{i-1}{N-1}\pi\right)]L,\ i = 1,2,\ldots,N, \quad (11a)$$
$$\theta_j = 0.5[1 - \cos\left(\frac{j-1}{M-1}\pi\right)]R,\ j = 1,2,\ldots,M \quad (11b)$$

The calculated values of frequency γ of applied heat flux for the thermal loads can be obtained in the heat conduction equation and referred to [12] for more details. Also the calculated values of vibration frequencyω_{mn}under free vibration ($f_1 = f_2 = \cdots = f_5 = 0$) can be obtained in the simply homogeneous equation and referred to [17] for more details.

The FGM constituent material 1 is SUS304 and constituent material 2 is Si_3N_4 that are applied for the GDQ numerical computations including the effect of advanced varied k_α. The dynamic convergence study of center displacement $w(L/2, 2\pi/2)$(mm) in thick FGM circular cylindrical shells is obtained firstly. Secondly, the amplitude of $w(L/2, 2\pi/2)$ for the thick FGM circular cylindrical shells is calculated. Also the normal stress σ_x(GPa) and shear stress $\sigma_{x\theta}$(GPa) are computed. Finally, the transient responses of $w(L/2, 2\pi/2)$ are presented for the thick FGM circular cylindrical shells in the following paragraphs.

 doi:10.20944/preprints202402.0142.v1

3.1. Advanced dynamic convergence study

The advanced dynamic convergence study of $w(L/2, 2\pi/2)$ in the thermal vibration of nonlinear TSDT of c_1= 0.925925/mm² and linear of c_1= 0/mm² for thick FGMs L/h^*= 10 with γ = 0.2618004/s and L/h^*= 5 with γ= 0.2618019/s, respectively at t= 6s, $L/R = 1$, h^*= 1.2mm, $h_1 = h_2$= 0.6mm, T= 100K, $\bar{T}_1$= 100K are presented in **Table 1**. The convergence values of $w(L/2, 2\pi/2)$ are calculated with the advanced nonlinear k_α and ω_{11} for three values of R_n. In the nonlinear L/h^* = 5 case of c_1= 0.925925/mm²: (a) for value of R_n= 0.5, k_α= -0.539419 and ω_{11}= 0.001731/s are obtained. (b) for value of R_n= 1, k_α= -0.922719 and ω_{11}= 0.001733/s are obtained. (c) for value of R_n= 2, k_α= 9.852628 and ω_{11}= 0.001735/s are obtained. In the linear L/h^* = 5 case of c_1= 0/mm²: (a) for value of R_n= 0.5, k_α= 1.136032 and ω_{11}= 0.002972/s are obtained. (b) for value of R_n= 1, k_α= 1.273499 and ω_{11}= 0.003009/s are obtained. (c) for value of R_n= 2, k_α= 1.317037 and ω_{11}= 0.002994/s are obtained. The error accuracy is 4.4e-06 for the nonlinear amplitude $w(L/2, 2\pi/2)$ of R_n= 0.5 and L/h^*= 10. The grid points with $N \times M$= 13×13 are in the very good convergence result for displacement and stress in the advanced thermal vibration of thick FGMs with advanced nonlinear k_α.

Table 1. Advanced convergence of FGM cylindrical shells with nonlinear varied k_α .

c_1(1/mm²)	L/h^*	GDQ method	$w(L/2, 2\pi/2)$(mm) at t= 6s		
		$N \times M$	R_n= 0.5	R_n= 1	R_n= 2
0.925925	10	7 × 7	1.128855	1.110114	0.460406
		9 × 9	1.130210	1.129728	0.460169
		11 × 11	1.130201	1.129750	0.460173
		13 × 13	1.130206	1.129744	0.460175
	5	7 × 7	0.085678	0.085501	0.097189
		9 × 9	0.085690	0.085513	0.097174
		11 × 11	0.085691	0.085513	0.097172
		13 × 13	0.085690	0.085513	0.097164
0	10	7 × 7	20.11788	19.25051	19.22559
		9 × 9	3.074959	3.096322	3.096179
		11 × 11	3.043667	3.072545	3.036793
		13 × 13	3.076776	3.077761	3.082854
	5	7 × 7	0.309435	0.309401	0.312130
		9 × 9	0.209839	0.289099	0.290058
		11 × 11	0.294196	0.288990	0.289848
		13 × 13	0.294207	0.289000	0.289840

3.2. Advanced time responses

The time responses of advanced $w(L/2, 2\pi/2)$ are obtained with the advanced nonlinear k_α values. The γ values are decreasing from γ=15.707960/s at t =0.1s to γ=0.523601/s at t =3.0s applied for L/h^*= 5, and from γ=15.707963/s at t =0.1s to γ=0.523599/s at t =3.0s applied for L/h^*= 10. The response of $w(L/2, 2\pi/2)$ values versus time t(s) are shown in **Figure 2** for nonlinear TSDT case with values c_1= 0.925925/mm², k_α= -3.535402 and for linear case with values c_1= 0/mm², k_α= 1.200860 in thick FGMs L/h^*= 5 and 10, respectively, $R_n = 1$, T=600K, $\bar{T}_1$=100K for t =0.1s-3.0s. The maximum value of $w(L/2, 2\pi/2)$ is 19.201795mm occurs at t = 0.1s for thick L/h^*= 5 with c_1= 0/mm² and γ = 15.707964/s. The maximum value of $w(L/2, 2\pi/2)$ is 224.052338mm at t = 0.1s for L/h^*= 10, c_1= 0/mm² and γ = 15.707963/s. The $w(L/2, 2\pi/2)$ values have the oscillating and decreasing tendencies in the case c_1= 0.925925/mm², amplitudes are decreasing with time in the case c_1= 0/mm² except at t= 2.6s for L/h^*= 5. The $w(L/2, 2\pi/2)$ values have the converging and decreasing tendencies in the c_1= 0.925925/mm² and c_1= 0/mm² for L/h^*= 10. The $w(L/2, 2\pi/2)$ values in c_1= 0/mm² are overestimated and greater than that in c_1= 0.925925/mm² at the corresponding time for the L/h^*= 10.

Preprints.org (www.preprints.org) | NOT PEER-REVIEWED | Posted: 2 February 2024 doi:10.20944/preprints202402.0142.v1

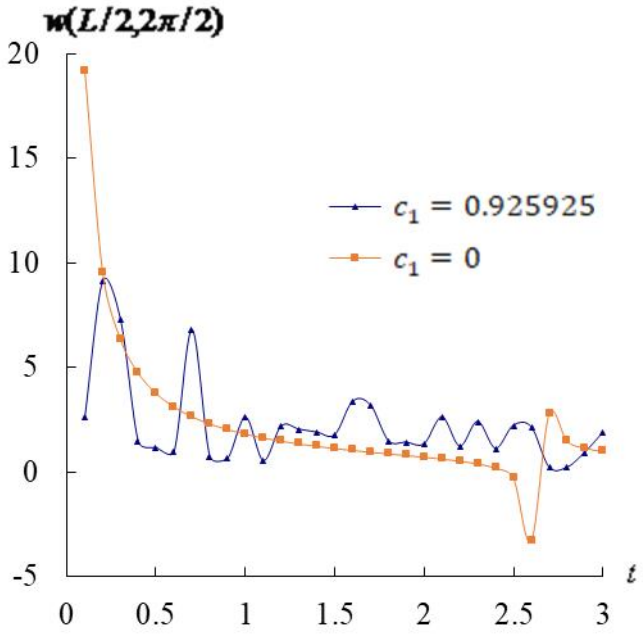

(**a**)

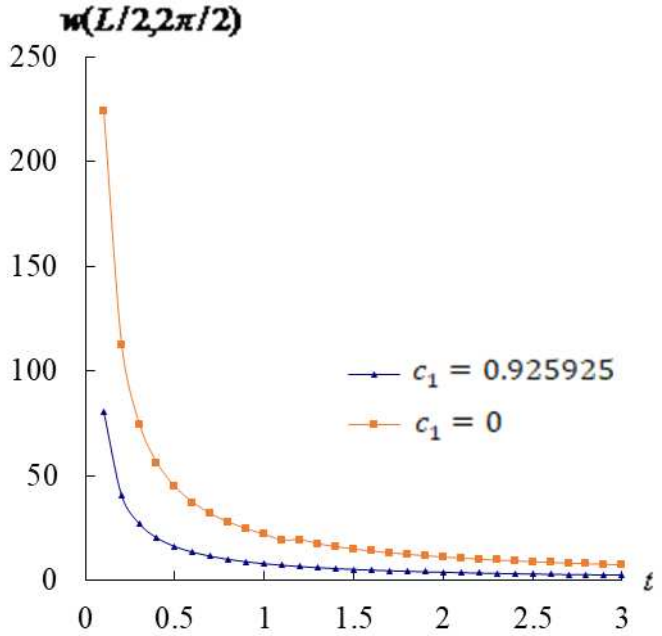

(**b**)

Figure 2. Advanced $w(L/2, 2\pi/2)$(mm) versus t(s): **(a)** L/h^*= 5, **(b)** L/h^*=10.

Figure 3 show the time responses of the dominated stress σ_x at center position of inner surface z = -0.5h^* for R_n= 1, L/h^*=5 and 10, c_1= 0.925925/mm². The σ_x maximum value is 1.8199E-03GPa occurs at t = 0.1s in the periods t =0.1s-3s for L/h^*= 5. The σ_x values have the oscillating and decreasing tendencies in c_1= 0.925925/mm² for L/h^*= 5. The σ_x values have the decreasing tendency in c_1= 0.925925/mm² for L/h^*= 10.

Preprints.org (www.preprints.org) | NOT PEER-REVIEWED | Posted: 2 February 2024 doi:10.20944/preprints202402.0142.v1

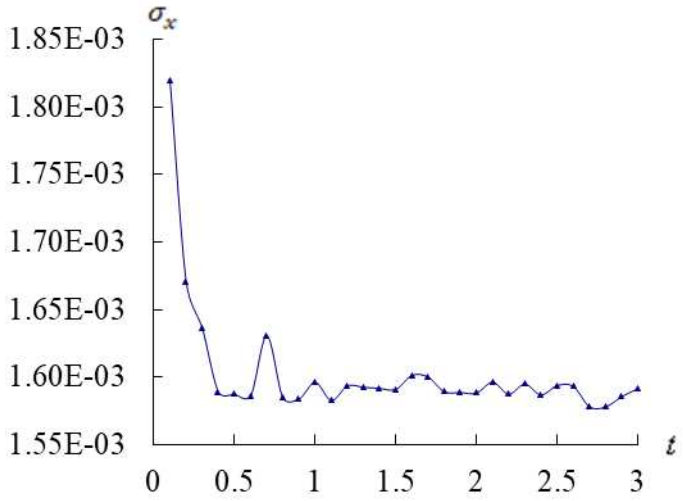

(**a**)

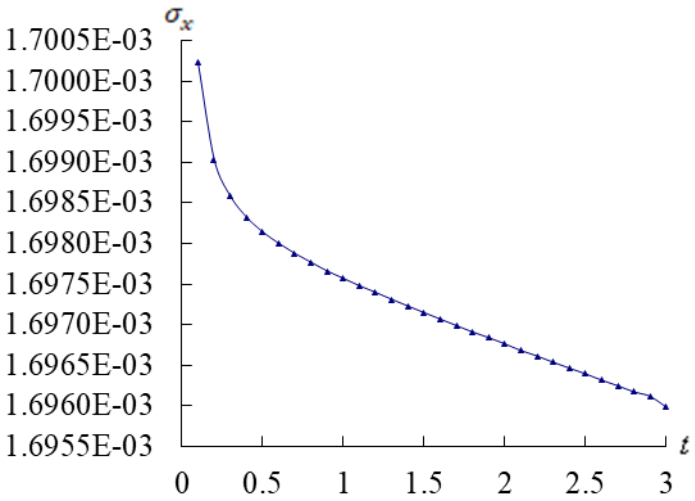

(**b**)

Figure 3. Advanced σ_x(GPa) versus t(s) **(a)** L/h^*= 5, **(b)** $L/h^* = 10$.

3.3. Effects of T and R_n on the advanced responses

Figure 4 shows the advanced response of $w(L/2, 2\pi/2)$ vs. T (100K, 600K and 1000K) and R_n at t = 0.1s in FGMs under $\bar{T}_1$=100K, c_1= 0.925925/mm² for L/h^*= 5 and 10. **Figure 4a** shows the values of $w(L/2, 2\pi/2)$ vs. T and R_n for the L/h^*= 5 case, the $w(L/2, 2\pi/2)$ maximum value is 9.064334mm in T=1000K for R_n= 0.1. The $w(L/2, 2\pi/2)$ value have the increasing tendency vs. T,

 doi:10.20944/preprints202402.0142.v1

the $w(L/2, 2\pi/2)$ of the L/h^*=5 cannot withstand for higher T=1000K. **Figure 4b** shows the values of $w(L/2, 2\pi/2)$ vs. T and R_n for the L/h^*= 10 case, they are almost located in the same curves except for R_n= 2. The $w(L/2, 2\pi/2)$ maximum value is 120.82637mm in T=1000K. The $w(L/2, 2\pi/2)$ value have the increasing tendency vs. T, the $w(L/2, 2\pi/2)$ of the L/h^*= 10 also cannot withstand for higher T=1000K at t = 0.1s.

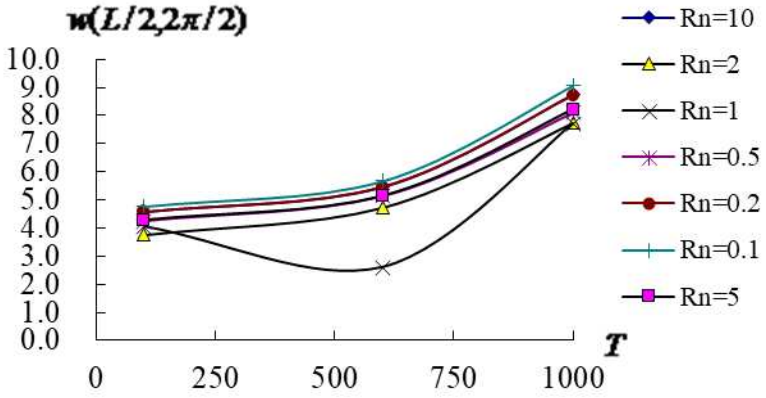

(**a**)

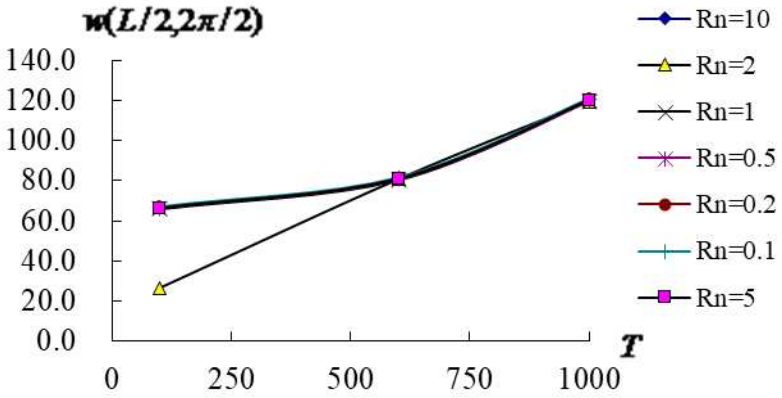

(**b**)

Figure 4. Advanced $w(L/2, 2\pi/2)$(mm) versus T(K) with R_n from 0.1 to 10: **(a)** L/h^*= 5, **(b)** L/h^*= 10.

Figure 5 shows the advanced normal stress σ_x at z = -0.5h^* vs. T and R_n at t = 0.1s in FGMs under $\bar{T}_1$=100K, c_1= 0.925925/mm² for thick L/h^*= 5 and 10. **Figure 5a** shows the σ_x values vs. T and R_n for the L/h^*= 5 case, the σ_x value have the increasing tendency from T=100K to T=600K and then decreasing tendency from T=600K to T=1000K. The σ_x maximum value is 0.001819GPa in T=600K for R_n= 1. The σ_x of the L/h^*= 5 can withstand for higher T=1000K. **Figure 5b** shows the values of σ_x vs. T and R_n for the L/h^*= 10 case, they are almost located in the same curves for all value of R_n, the σ_x value vs. T have the increasing tendency from T=100K to T=600K and then all

Preprints.org (www.preprints.org) | NOT PEER-REVIEWED | Posted: 2 February 2024 doi:10.20944/preprints202402.0142.v1

decreasing tendency from T=600K to T=1000K. The σ_x maximum value is 0.001761GPa in T=600K. The dominated stress σ_x of the L/h^*= 10 also can withstand for higher T=1000K.

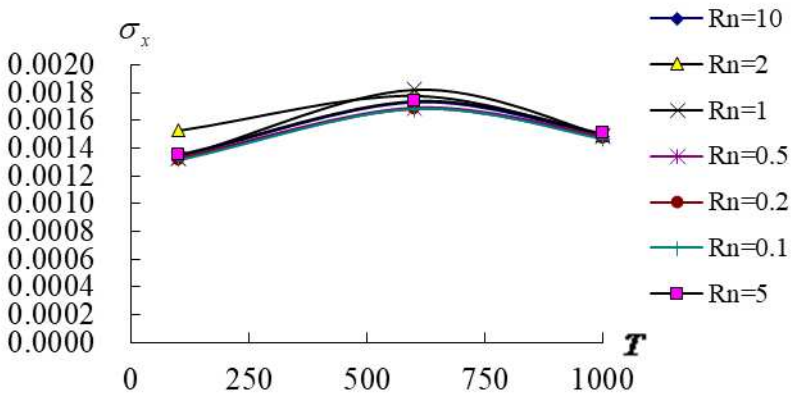

(**a**)

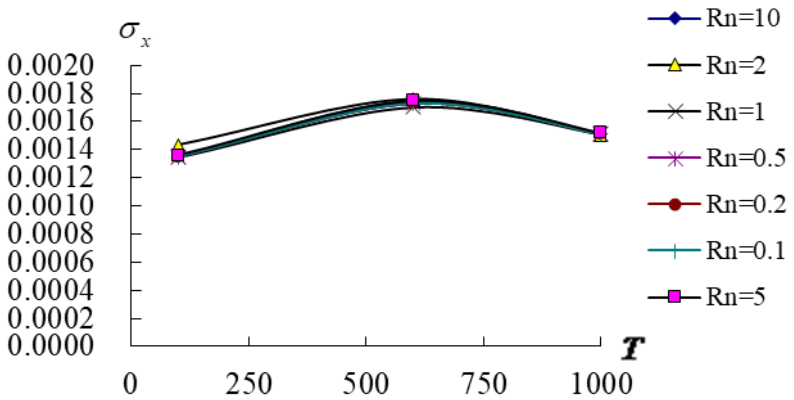

(**b**)

Figure 5. Advanced σ_x(GPa) versus T (K): **(a)** L/h^*= 5, **(b)** L/h^*= 10.

3.4. Advanced transient responses

The advanced transient responses of $w(L/2, 2\pi/2)$ are presented with c_1= 0.925925/mm² for L/h^*= 10 and fixed ω_{11}= 0.000592/s as shown in **Figure 6**. Also used the fixed values of applied heat flux γ, $L/R = 1$, h^*= 1.2mm, $h_1 = h_2$= 0.6mm, $R_n = 1$, advanced varied values of k_α= -3.535402, T=600K, $\bar{T}_1$=100K for period t = 0.002s-0.025s and time step 0.001s is used. **Figure 6a** shows the compared transient response of $w(L/2, 2\pi/2)$ for L/h^*= 10 with super value γ= 284314.1/s and high value γ= 785.3982/s. The transient values of $w(L/2, 2\pi/2)$ vs. higher γ are all oscillating and decreasing for L/h^*= 10. **Figure 6b** shows the compared transient response of $w(L/2, 2\pi/2)$ for L/h^*= 10 with lower values γ= 15.707963/s and γ= 0.523599/s. The transient values of $w(L/2, 2\pi/2)$ vs. lower γ are all rapid converging for L/h^*= 10.

Preprints.org (www.preprints.org) | NOT PEER-REVIEWED | Posted: 2 February 2024 doi:10.20944/preprints202402.0142.v1

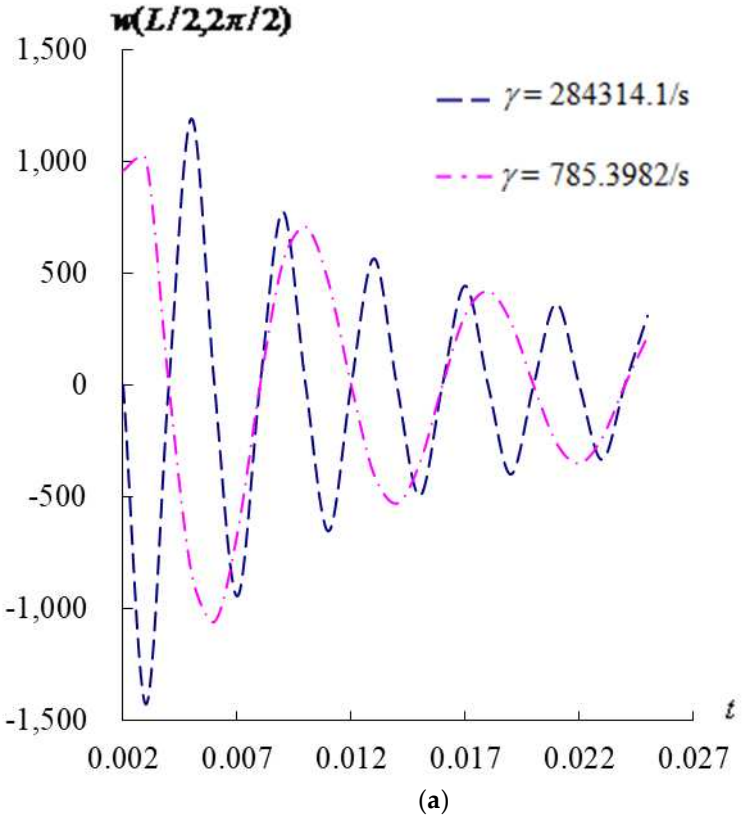

(**a**)

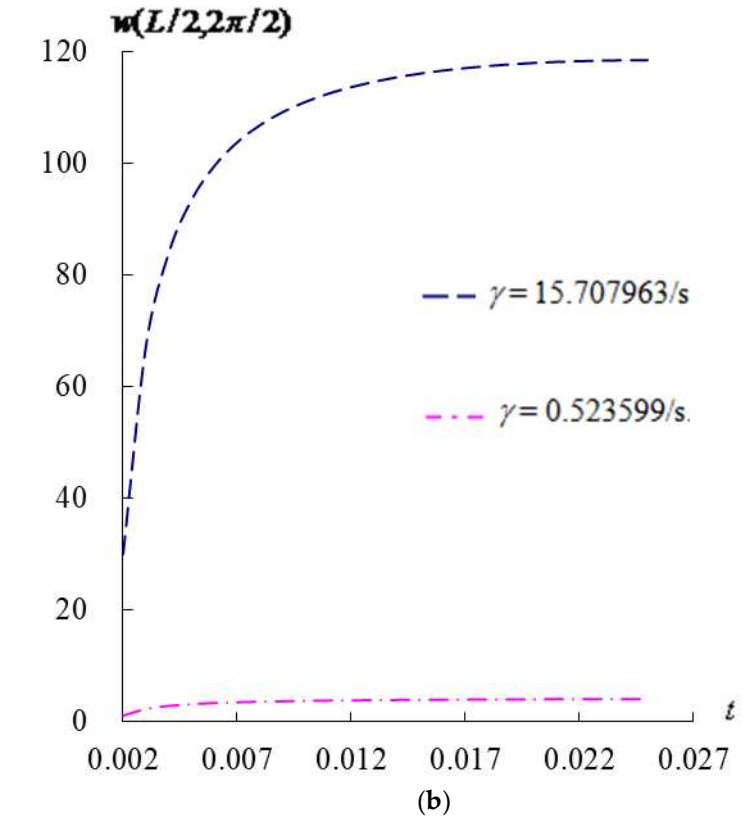

(**b**)

Figure 6. Advanced transient $w(L/2, 2\pi/2)$(mm) vs. t(s) for L/h^*= 10: **(a)** γ= 284314.1/s and 785.3982/s, **(b)** γ= 15.707963/s and 0.523599/s.

 doi:10.20944/preprints202402.0142.v1

4. Conclusions

The advanced displacements and stresses of numerical GDQ results are presented for the thick FGM circular cylindrical shells. The most important parameter effects of nonlinear shear coefficient is considered. The second important parameter effects of c_1 coefficient in TSDT is also considered. The advanced $w(L/2, 2\pi/2)$ values in c_1= 0/mm² are overestimated and greater than that in c_1= 0.925925/mm² at the corresponding time for the L/h^*= 10. The advanced $w(L/2, 2\pi/2)$ values of the L/h^*=5 and 10 can't withstand in higher T=1000K. The advanced σ_x values of the L/h^*= 5 and 10 can withstand in higher T=1000K of environment for thick FGMs at t = 0.1s. The advanced transient values of $w(L/2, 2\pi/2)$ vs. lower frequency of applied heat flux are all rapid converging.

Author Contributions: For research articles with only one author.

Funding: There is no funder for this study.

Data Availability Statement: In the manuscript completely mentioned the data used to generate the figures and tables. Data are all available on request. Declare all the data are generated by the author, also data are openly available.

Acknowledgments: The author expresses his thanks to the people helping with this work, and acknowledge the valuable suggestions from the peer reviewers.

Conflicts of Interest: The authors declare that they have no conflict of interest.

Appendix A

The elements of **HM**, **EM**, **FM**, **AM**, **BM**, **KE** and **FQ** are expressed as follows,

$\mathbf{HM} = [\mathrm{HM}_{ij}]$ is a 5 by 5 matrix, in which elements of $\mathrm{HM}_{11} = \mathrm{HM}_{12} = \ldots = \mathrm{HM}_{15} = \mathrm{HM}_{21} = \mathrm{HM}_{22} = \ldots = \mathrm{HM}_{25} = \mathrm{HM}_{41} = \mathrm{HM}_{42} = \ldots = \mathrm{HM}_{45} = \mathrm{HM}_{51} = \mathrm{HM}_{52} = \ldots = \mathrm{HM}_{55} = 0$, $\mathrm{HM}_{31} = -c_1{}^2 H_{11}$, $\mathrm{HM}_{32} = -4c_1{}^2 H_{16}$, $\mathrm{HM}_{33} = -2c_1{}^2 H_{12} - 4c_1{}^2 H_{66}$, $\mathrm{HM}_{34} = -4c_1{}^2 H_{26}$ and $\mathrm{HM}_{35} = -c_1{}^2 H_{22}$. (A1)

$\mathbf{EM} = [\mathrm{EM}_{ij}]$ is a 5 by 12 matrix in which elements of $\mathrm{EM}_{11}=\mathrm{EM}_{12}=\ldots=\mathrm{EM}_{18}=\mathrm{EM}_{21}=\mathrm{EM}_{22}=\ldots=\mathrm{EM}_{28}=\mathrm{EM}_{39}=\mathrm{EM}_{310}=\ldots=\mathrm{EM}_{312}=\mathrm{EM}_{41}=\mathrm{EM}_{42}=\ldots=\mathrm{EM}_{48}=\mathrm{EM}_{51}=\mathrm{EM}_{52}=\ldots=\mathrm{EM}_{58}=0$, $\mathrm{EM}_{19} = -c_1 E_{11}$, $\mathrm{EM}_{110} = -3c_1 E_{16}$, $\mathrm{EM}_{111} = -c_1 E_{12} - -2c_1 E_{66}$, $\mathrm{EM}_{112} = -c_1 E_{26}$, $\mathrm{EM}_{29} = -c_1 E_{16}$, $\mathrm{EM}_{210} = -c_1 E_{12} - 2c_1 E_{66}$, $\mathrm{EM}_{211} = -3c_1 E_{26}$, $\mathrm{EM}_{212} = -c_1 E_{22}$, $\mathrm{EM}_{31} = c_1 E_{11}$, $\mathrm{EM}_{32} = 3c_1 E_{16}$, $\mathrm{EM}_{33} = c_1 E_{12} + 2c_1 E_{66}$, $\mathrm{EM}_{34} = c_1 E_{26}$, $\mathrm{EM}_{35} = c_1 E_{16}$, $\mathrm{EM}_{36} = c_1 E_{12} + 2c_1 E_{66}$, $\mathrm{EM}_{37} = 3c_1 E_{26}$, $\mathrm{EM}_{38} = c_1 E_{22}$, $\mathrm{EM}_{49} = -c_1 F_{11} + c_1{}^2 H_{11}$, $\mathrm{EM}_{410} = -3c_1 F_{16} + 3c_1{}^2 H_{16}$, $\mathrm{EM}_{411} = -c_1 F_{12} + c_1{}^2 H_{12} - 2c_1 F_{66} + 2c_1{}^2 H_{66}$, $\mathrm{EM}_{412} = -c_1 F_{26} + c_1{}^2 H_{26}$, $\mathrm{EM}_{59} = -c_1 F_{16} + c_1{}^2 H_{16}$, $\mathrm{EM}_{510} = -2c_1 F_{66} + 2c_1{}^2 H_{66} - 2c_1 F_{12} + 2c_1{}^2 H_{12}$, $\mathrm{EM}_{511} = -3c_1 F_{26} + 3c_1{}^2 H_{26}$ and $\mathrm{EM}_{512} = -c_1 F_{22} + c_1{}^2 H_{22}$. (A2)

$\mathbf{FM} = [\mathrm{FM}_{ij}]$ is a 5 by 8 matrix, in which elements of $\mathrm{FM}_{11} = \mathrm{FM}_{12} = \ldots = \mathrm{FM}_{18} = \mathrm{FM}_{21} = \mathrm{FM}_{22} = \ldots = \mathrm{FM}_{28} = \mathrm{FM}_{41} = \mathrm{FM}_{42} = \ldots = \mathrm{FM}_{48} = FM_{51} = FM_{52} = \ldots = FM_{58} = 0$, $FM_{31} = c_1 F_{11} - c_1{}^2 H_{11}$, $FM_{32} = 3c_1 F_{16} - 3c_1{}^2 H_{16}$, $\mathrm{FM}_{33} = 2c_1 F_{66} - 2c_1{}^2 H_{66} + c_1 F_{12} - c_1{}^2 H_{12}$, $\mathrm{FM}_{34} = c_1 F_{26} - c_1{}^2 H_{26}$, $\mathrm{FM}_{35} = c_1 F_{16} - c_1{}^2 H_{16}$, $\mathrm{FM}_{36} = c_1 F_{12} - c_1{}^2 H_{12} + 2c_1 F_{66} - 2c_1{}^2 H_{66}$, $\mathrm{FM}_{37} = 3c_1 F_{26} - 3c_1{}^2 H_{26}$, $\mathrm{FM}_{38} = c_1 F_{22} - c_1{}^2 H_{22}$. (A3)

$\mathbf{AM} = [\mathrm{AM}_{ij}]$ is a 5 by 9 matrix, in which elements of $\mathrm{AM}_{11}=A_{11}$, $\mathrm{AM}_{12}=2A_{16}$, $\mathrm{AM}_{13}=A_{66}$, $\mathrm{AM}_{14}=A_{16}$, $\mathrm{AM}_{15}=A_{12}+A_{66}$, $\mathrm{AM}_{16}=A_{26}$, $\mathrm{AM}_{17}=\mathrm{AM}_{18}=\mathrm{AM}_{19}=0$, $\mathrm{AM}_{21}=A_{16}$, $\mathrm{AM}_{22}=A_{12}+A_{66}$, $\mathrm{AM}_{23}=A_{26}$, $\mathrm{AM}_{24}=A_{66}$, $\mathrm{AM}_{25}=2A_{26}$, $\mathrm{AM}_{26}=A_{22}$, $\mathrm{AM}_{27}=\mathrm{AM}_{28}=\mathrm{AM}_{29}=0$, $\mathrm{AM}_{31}=\mathrm{AM}_{32}=\ldots=\mathrm{AM}_{36}=0$, $\mathrm{AM}_{37} = -3c_1(2D_{55}-3c_1F_{55}) + A_{55} + c_1{}^2 I_6 \frac{\partial^2}{\partial t^2}$, $\mathrm{AM}_{38} = -6c_1(2D_{45}-3c_1F_{45})$ +2 A_{45}, $\mathrm{AM}_{39} = -3c_1(2D_{44}-3c_1F_{44}) + A_{44} + c_1{}^2 I_6 \frac{\partial^2}{\partial t^2}$, $\mathrm{AM}_{41} = B_{11}-c_1E_{11}$, $\mathrm{AM}_{42} = 2B_{16}-2c_1E_{16}$, $\mathrm{AM}_{43} = B_{66}-c_1E_{66}$, $\mathrm{AM}_{44} = B_{16}-c_1E_{16}$, $\mathrm{AM}_{45} = B_{12} + B_{66}-c_1E_{12} \quad -c_1E_{66}$, $\mathrm{AM}_{46} = B_{26}-c_1E_{26}$, $\mathrm{AM}_{47}=\mathrm{AM}_{48}=\mathrm{AM}_{49}=0$, $\mathrm{AM}_{51} = B_{16}-c_1E_{16}$, $\mathrm{AM}_{52} = B_{12} + B_{66}-c_1E_{12} \quad -c_1E_{66}$, $\mathrm{AM}_{53} = B_{26}-c_1E_{26}$, $\mathrm{AM}_{54} = B_{66}-c_1E_{66}$, $\mathrm{AM}_{55} = 2B_{26}-2c_1E_{26}$, $\mathrm{AM}_{56} = B_{22}-c_1E_{22}$ and $\mathrm{AM}_{57}=\mathrm{AM}_{58}=\mathrm{AM}_{59}=0$. (A4)

$\mathbf{BM} = [\mathrm{BM}_{ij}]$ is a 5 by 6 matrix, in which elements of $\mathrm{BM}_{11}=B_{11}-c_1E_{11}$, $\mathrm{BM}_{12} = 2B_{16}-2c_1E_{16}$, $\mathrm{BM}_{13} = B_{66}-c_1E_{66}$, $\mathrm{BM}_{14} = B_{16}-c_1E_{16}$, $\mathrm{BM}_{15} = B_{12} + B_{66}-c_1E_{12}-c_1E_{66}$, $\mathrm{BM}_{16} = B_{26}-c_1E_{26}$, $\mathrm{BM}_{21} = B_{16}-c_1E_{16}$, $\mathrm{BM}_{22} = B_{12} + B_{66}-c_1E_{12}-c_1E_{66}$, $\mathrm{BM}_{23} = B_{26}-c_1E_{26}$, $\mathrm{BM}_{24} = B_{66}-c_1E_{66}$,

 doi:10.20944/preprints202402.0142.v1

$BM_{25} = 2B_{16} - 2c_1E_{16}$, $BM_{26} = B_{22} - c_1E_{22}$, BM_{31}=BM_{32}=…=BM_{36}=0, $BM_{41} = D_{11} - 2c_1F_{11} + {c_1}^2H_{11}$, $BM_{42} = 2D_{16} - 4c_1F_{16} + 2{c_1}^2H_{16}$, $BM_{43} = D_{66} - 2c_1F_{66} + {c_1}^2H_{66}$, $BM_{44} = D_{16} - 2c_1F_{16} + {c_1}^2H_{16}$, $BM_{45} = D_{12} + D_{66} - 2c_1F_{12} + {c_1}^2H_{12} - 2c_1F_{66} + {c_1}^2H_{66}$, $BM_{46} = D_{26} - 2c_1F_{26} + {c_1}^2H_{26}$, $BM_{51} = D_{16} - 2c_1F_{16} + {c_1}^2H_{16}$, $BM_{52} = D_{12} + D_{66} - 2c_1F_{12} + {c_1}^2H_{12} - 2c_1F_{66} + {c_1}^2H_{66}$, $BM_{53} = D_{26} - 2c_1F_{26} + {c_1}^2H_{26}$, $BM_{54} = D_{66} - 2c_1F_{66} + {c_1}^2H_{66}$, $BM_{55} = 2D_{26} - 4c_1F_{26} + 2{c_1}^2H_{26}$ and $BM_{56} = D_{22} - 2c_1F_{22} + {c_1}^2H_{22}$. (A5)

$\mathbf{KE} = [KE_{ij}]$ is a 5 by 10 matrix, in which elements of KE_{11}= KE_{12}=…=KE_{14}=0, $KE_{15}=c_1I_3\frac{\partial^2}{\partial t^2}$, KE_{16}= KE_{17}=…=KE_{110}=0, KE_{21}= KE_{22}=…=KE_{25}=0, $KE_{26}=c_1I_3\frac{\partial^2}{\partial t^2}$, KE_{27}= KE_{28}=…=KE_{110}=0, KE_{31}= $-c_1I_3\frac{\partial^2}{\partial t^2} - \frac{u_0}{R}(A_{55} - 3c_1D_{55})$, $KE_{32} = -\frac{u_0}{R}(A_{45} - 3c_1D_{45})$, $KE_{33} = -\frac{v_0}{R}(A_{45} - 3c_1D_{45})$, $KE_{34} = -c_1I_3\frac{\partial^2}{\partial t^2} - \frac{v_0}{R}(A_{44} - 3c_1D_{44})$, KE_{35} = KE_{36} =0, $KE_{37} = A_{55} - 6c_1D_{55} + 9{c_1}^2F_{55} - c_1J_4\frac{\partial^2}{\partial t^2}$, $KE_{38} = A_{44} - 6c_1D_{44} + 9{c_1}^2F_{44} - c_1J_4\frac{\partial^2}{\partial t^2}$, KE_{41}= KE_{42}=…=KE_{44}=0, KE_{45}= $-A_{55} + 6c_1D_{55} - 9{c_1}^2F_{55} + c_1J_4\frac{\partial^2}{\partial t^2}$, $KE_{46} = -A_{45} + 6c_1D_{45} - 9{c_1}^2F_{45}$, KE_{47} = KE_{48} =…= KE_{410} =0, KE_{51} = KE_{52} =…= KE_{54} =0, $KE_{55} = -A_{45} + 6c_1D_{45} - 9{c_1}^2F_{45}$, $KE_{56} = -A_{44} + 6c_1D_{44} - 9{c_1}^2F_{44} + c_1J_4\frac{\partial^2}{\partial t^2}$ and KE_{57}= KE_{58}=…=KE_{510}=0. (A6)

$\mathbf{FQ} = [FQ_{ij}]$ is a 5 by 5 matrix, in which elements of $FQ_{11} = -I_0\frac{\partial^2}{\partial t^2}$, $FQ_{12} = FQ_{13} = 0$, $FQ_{14} = -J_1\frac{\partial^2}{\partial t^2}$, $FQ_{15} = 0$, $FQ_{21} = 0$, $FQ_{22} = -I_0\frac{\partial^2}{\partial t^2}$, $FQ_{23} = FQ_{24} = 0$, $FQ_{25} = -J_1\frac{\partial^2}{\partial t^2}$, $FQ_{31} = FQ_{32} = 0$, $FQ_{33} = -I_0\frac{\partial^2}{\partial t^2}$, $FQ_{34} = FQ_{35} = 0$, $FQ_{41} = -J_1\frac{\partial^2}{\partial t^2} - \frac{1}{R}(-A_{55} + 3c_1D_{55})$, $FQ_{42} = -\frac{1}{R}(-A_{45} + 3c_1D_{45})$, $FQ_{43} = 0$, $FQ_{44} = -A_{55} + 6c_1D_{55} - 9{c_1}^2F_{55} + K_2\frac{\partial^2}{\partial t^2}$, $FQ_{45} = -A_{45} + 6c_1D_{45} - 9{c_1}^2F_{45}$, $FQ_{51} = -\frac{1}{R}(-A_{45} + 3c_1D_{45})$, $FQ_{52} = -J_1\frac{\partial^2}{\partial t^2} - \frac{1}{R}(-A_{44} + 3c_1D_{44})$, $FQ_{53} = 0$, $FQ_{54} = -A_{45} + 6c_1D_{45} - 9{c_1}^2F_{45}$ and $FQ_{55} = -A_{44} + 6c_1D_{44} - 9{c_1}^2F_{44} + K_2\frac{\partial^2}{\partial t^2}$. A(7)

References

1. Abouelregal, A.E.; Marin, M.; Abusalim, S.M. An investigation into thermal vibrations caused by a moving heat supply on a spinning functionally graded isotropic piezoelectric bounded rod. Mathematics **2023**, 11, 1739, 1–17.
2. Tang, Z.; Hu, J.; Li, Z. A fast reduced-order model for radial integration boundary element method based on proper orthogonal decomposition in the non-uniform coupled thermoelastic problems. Mathematics **2023**, 11, 3870, 1–29.
3. Chen, Z.; Wang, A.; Qin, B.; Wang, Q.; Zhong, R. Investigation on vibration of the functionally graded material–stepped cylindrical shell coupled with annular plate in thermal environment. Journal of Low Frequency Noise, Vibr. and Acti. Cont. **2022**, 41(1), 85–111.
4. Ramteke, P.M.; Kumar, V.; Sharma, N.; Panda, S.K. Geometrical nonlinear numerical frequency prediction of porous functionally graded shell panel under thermal environment. Int. J. of Non-Line. Mech. **2022**, 143, 104041, 1–14.
5. Saeedi, S.; Kholdi, M.; Loghman, A.; Ashrafi, H.; Aref, M. Thermo-elasto-plastic analysis of thick-walled cylinder made of functionally graded materials using successive approximation method. Int. J. of Pres. Vess. and Pipi. **2021**, 194, 104481, 1–12.
6. Gee, A.; Hashemi, S.M. Undamped Free Vibration Analysis of Functionally Graded Beams: A Dynamic Finite Element Approach, Appl. Mech. **2022**, 3(4), 1223–1239.
7. Khoshgoftar, M.J. Second order shear deformation theory for functionally graded axisymmetric thick shell with variable thickness under non-uniform pressure. Thin-Wall. Struct. **2019**, 144, 106286, 1–7.
8. Trinh, M.C.; Kim, S.E. Nonlinear stability of moderately thick functionally graded sandwich shells with double curvature in thermal environment. Aero. Sci. and Tech. **2019**, 84, 672–685.
9. Nejad, M.Z.; Jabbari, M.; Hadi, A. A review of functionally graded thick cylindrical and conical shells. JCAMECH **2017**, 48, issue 2, 357–370.
10. Hong, C.C. GDQ computation for thermal vibration of thick FGM plates by using third-order shear deformation theory. Mater. Sci. and Eng. B **2023**, 294, 116208, 1–22.
11. Hong, C.C. Advanced dynamic thermal vibration of laminated FGM plates with simply homogeneous equation by using TSDT and nonlinear varied shear coefficient. Appl. Sci. **2022**, 12, 11776, 1–14.
12. Hong, C.C. Thermal vibration of thick FGM circular cylindrical shells by using TSDT. Mater. Plus **2022**, 1, issue 1, 1–10.
13. Hong, C.C. Advanced dynamic thermal vibration of thick FGM plates-cylindrical shells. Ocean Eng. **2022**, 266, 112701, 1–16.

 doi:10.20944/preprints202402.0142.v1

14. Lee, S.J.; Reddy, J.N.; Rostam-Abadi, F. Transient analysis of laminated composite plates with embedded smart-material layers. Fin. Elem. in Anal. and Des. **2004**, 40, 463–483.
15. Whitney, J.M. Structural analysis of laminated anisotropic plates. Lancaster: Pennsylvania, USA, Technomic Publishing Company, Inc. 1987.
16. Hong, C.C. Thermal vibration of magnetostrictive functionally graded material shells by considering the varied effects of shear correction coefficient. Int. J. of Mech. Sci. **2014**, 85, 20–29.
17. Hong, C.C. Advanced frequency study of thick FGM cylindrical shells by using TSDT and nonlinear shear. Mat. Plus **2023**, 2, issue 2, 1–11.